

- Pitts, *ibid.*, p. 1623; F. F. Fenter, F. Caloz, M. J. Rossi, *J. Phys. Chem.* **98**, 9801 (1994); W. Behnke, V. Scheer, C. Zetzsch, *J. Aerosol Sci.* **24**, S115 (1993); Y. Mamane and J. Gottlieb, *ibid.* **21**, S225 (1990); B. J. Finlayson-Pitts, M. J. Ezell, J. N. Pitts Jr., *Nature* **337**, 241 (1989); F. Bruynseels and R. Van Grieken, *Atmos. Environ.* **19**, 1969 (1985).
14. To confirm that the particles selected are in fact sea salt, the ratio of the relative intensities of Na⁺ and K⁺ can be compared to that in sea water with use of the empirical relative sensitivity factor (RSF) measured by D. S. Gross, M. E. Gälli, and K. A. Prather (in preparation). Although the sea-salt particles are identified strictly on the basis of composition, they also have a characteristic aerodynamic diameter greater than 1.0 μm, which helps corroborate their source.
 15. Previous models of urban aerosol properties as a computational approximation generally treat all atmospheric particles of the same size as having the same chemical composition and thus cannot differentiate sea-salt particles explicitly from other particles of similar size. See (10) for a discussion of the representation of particle size and composition in modeling calculations.
 16. W. R. Goodin *et al.*, *J. Appl. Meteorol.* **18**, 761 (1979).
 17. Within the model, the air parcels begin over the ocean with regional background aerosol as measured during the Southern California Air Quality Survey (SCAQs) experiments conducted in Los Angeles in 1987, and they pick up sea-salt aerosol at the concentrations measured during SCAQS as they cross the surf zone at the coastline (10). As the air parcels pass over land, emissions from the urban sources in Los Angeles are inserted into the model on the basis of the 1996 emissions inventory maintained by the South Coast Air Quality Management District, modified according to the procedures of A. Eldering and G. R. Cass [*J. Geophys. Res.* **101**, 19343 (1996)]. The same initial conditions for sea salt are used for each trajectory even though there must be hour-to-hour variations; for that reason, we do not expect exact agreement between predictions and observations at Long Beach.
 18. The upper limit of 2.5 μm for particle diameter was chosen as the best match between the size bins used to track particles in the model calculation and the inherent transmission efficiency of the ATOFMS inlet nozzle, which transmits particles below ~3 μm with high efficiency.
 19. We thank R. A. Carlin, D.-Y. Liu, C. A. Noble, P. J. Silva, and S. H. Wood for assistance with ATOFMS data acquisition. In addition, we are grateful to R. Williams and M. Berg at California State University at Long Beach and B. Gill at California State University at Fullerton for use of their facilities. Funding (University of California at Riverside) was provided by the California Air Resources Board (ARB contract 95-305). Funding (California Institute of Technology) was provided by grants from the U.S. Environmental Protection Agency (EPA grant R824970-01-0) and from the California Institute of Technology Center for Air Quality Analysis.

5 November 1997; accepted 20 January 1998

Atmospheric Radiocarbon Calibration to 45,000 yr B.P.: Late Glacial Fluctuations and Cosmogenic Isotope Production

H. Kitagawa* and J. van der Plicht

More than 250 carbon-14 accelerator mass spectrometry dates of terrestrial macrofossils from annually laminated sediments from Lake Suigetsu (Japan) provide a first atmospheric calibration for almost the total range of the radiocarbon method (45,000 years before the present). The results confirm the (recently revised) floating German pine chronology and are consistent with data from European and marine varved sediments, and combined uranium-thorium and carbon-14 dating of corals up to the Last Glacial Maximum. The data during the Glacial show large fluctuations in the atmospheric carbon-14 content, related to changes in global environment and in cosmogenic isotope production.

from Lake Suigetsu (35°35'N, 135°53'E) near the coast of the Sea of Japan (11). The lake is 10 km around the perimeter and covers an area of 4.3 km². It is a typical kettle-type lake with a nearly constant depth at the center, ~34 m deep. A 75-m-long continuous core (Lab. code, SG) and four short piston cores were taken from the center of the lake in 1991 and 1993. The sediments are laminated in nearly the entire core sections and are dominated by dark-colored clay with white layers resulting from spring-season diatom growth. The seasonal changes in the depositions are preserved in the clay as thin laminations or varves. The sedimentation or annual varve thickness is relatively uniform, typically 1.2 mm/year during the Holocene and 0.61 mm/year during the Glacial. The bottom age of the SG core is estimated to be older than 100,000 years, close to the beginning of the last interglacial period.

To reconstruct the calendar time scale, we counted varves, based on gray-scale image analyses of digital pictures, in a 10.43- to 30.45-m-deep section, producing a 29,100-year-long floating chronology. Because we estimated the varve chronology of older than ~20,000 yr B.P. (19-m depth of SG core) by counting in a single core section, the error of the varve counting increases with depth, and the accumulated error at 40,000 cal yr B.P. would be less than ~2000 years, assuming no break in the sediment (12).

The ¹⁴C/¹²C and ¹³C/¹²C ratios of more than 250 terrestrial macrofossils (leaves, twigs, and insect wings) in the sediments were measured by accelerator mass spectrometry (AMS) at the Groningen AMS facility (13), after proper sample pretreatment (14).

The floating varve chronology was connected to the old part of the absolute tree-ring chronology (2, 15) by ¹⁴C wiggle matching (16), resulting in an absolute calendar age covering the time span from 8830 to 37,930

The atmospheric ¹⁴C content (expressed in Δ¹⁴C) (1) is sensitive to geomagnetic field strength and solar fluctuations (also through magnetic effects) as well as rearrangements in equilibrium between the major C reservoirs (atmosphere, ocean, and biosphere). Detailed calibration of the radiocarbon time scale into the glacial period is critical for accurate dating and a better understanding of changes in the Earth system.

Radiocarbon calibration can be performed by ¹⁴C dating of samples that can also be dated by an independent, preferably absolute dating method. The ideal samples for this purpose are tree rings, which can be dated by dendrochronology. Dendro-calibrations with (for the most part) 20-year tree-ring resolution have been obtained for almost the complete Holocene, back to about 7900 B.C. for the absolute chronology

and to about 9400 B.C. including a matched floating tree-ring curve (2).

Beyond the range of tree rings, calibration has been problematic. Radiocarbon dates of terrestrial macrofossils from annually laminated sediments can potentially provide a high-resolution record of atmospheric ¹⁴C changes. However, varve chronologies have been revised several times (3). At present, calibration data from glacial varves provide a consistent data set back to about 11,000 B.C. (4–6). In addition, a marine calibration curve for the Late Glacial period is obtained by combined ¹⁴C and U-series dates of corals (7, 8) and ¹⁴C measurements on foraminifera from varved marine sediments (9). Because these data are for marine materials, they have to be corrected for the apparent ¹⁴C age of the surface oceans, known as the reservoir effect.

Here we present a high-resolution atmospheric radiocarbon calibration from annually laminated sediments for the total range of the radiocarbon dating method [$<45,000$ cal yr B.P. (10)]. The sediments were taken

H. Kitagawa, International Research Center for Japanese Studies, 3-2, Goryo Oeyama-cho, Nishikyō-ku, Kyoto, 610-1192 Japan.

J. van der Plicht, Centre for Isotope Research, Nijenborgh 4, 9747AG Groningen, Netherlands.

*To whom correspondence should be addressed.

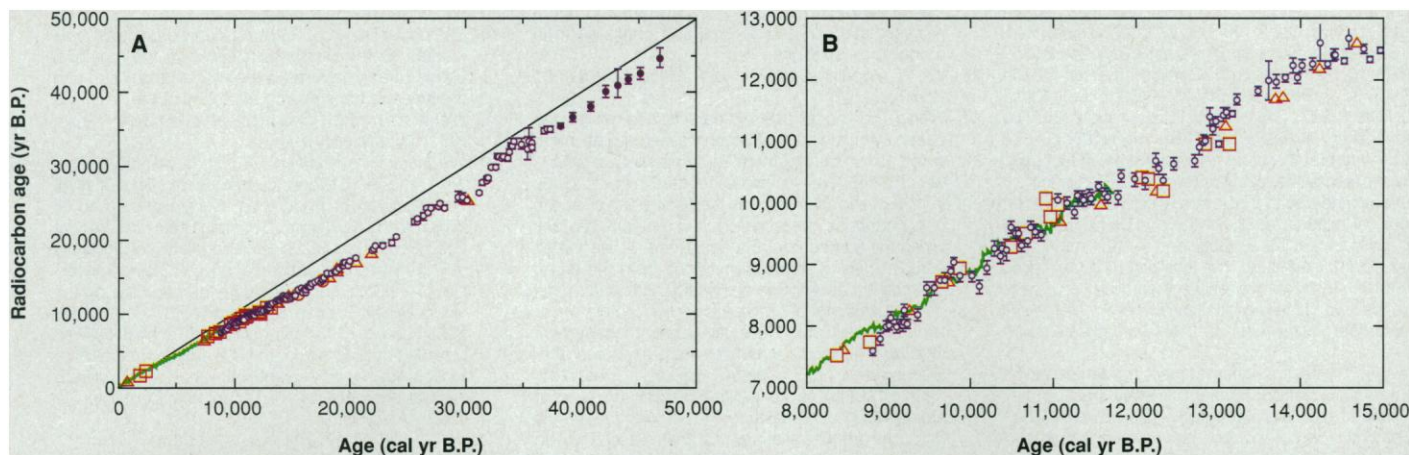


Fig. 1. (A) Radiocarbon calibration up to 45,000 yr B.P. reconstructed from annually laminated sediments of Lake Suigetsu, Japan. The small circles with 1σ error represent the ^{14}C ages against varve ages. For the oldest eight points (>38,000 years, filled circles), we assumed a constant sedimentation during the Glacial period. The green symbols correspond to the tree-ring calibration (2, 15), and the large red symbols represent

calibration by combined ^{14}C and U-Th dating of corals from Papua New Guinea (squares) (8), Mururoa (circles), and Barbados (triangles) (7). The line indicates that radiocarbon age equals calibrated age. **(B)** Agreement of the 29,000-year floating varve chronology with absolute and recently revised floating German pine chronology, and radiocarbon calibration during the deglaciation.

cal yr B.P. (17). The age beyond 37,930 cal yr B.P. is obtained by assuming a constant sedimentation in the Glacial.

The combined AMS ^{14}C and varve ages provide an extension of dendro-calibration range (Fig. 1). The features in the data overlapping the absolute tree-ring record agree very well, and our varve chronology also supports the recent revision of the floating German pine chronology, which was shifted by 160 years to older ages (6, 15). Beyond the range of the dendro-calibration (~11,700 cal yr B.P.), there is also general agreement with the European sediments (5, 6) as well as with marine calibrations (7–9).

The detailed record in atmospheric $\Delta^{14}\text{C}$ during the deglaciation shows millennium-scale fluctuations superimposed on a long-term increasing trend into the past resulting from a decreasing geomagnetic intensity as reconstructed from geomagnetic records (18) (Fig 2). The long-term increase is also consistent with a model-generated

estimate of atmospheric $\Delta^{14}\text{C}$ increase (19), on the basis of ^{10}Be flux records (20). Abrupt $\Delta^{14}\text{C}$ decreases correspond to radiocarbon plateaus in the calibration curve. Near (a few centuries after) the onset of the Younger Dryas (YD), the $\Delta^{14}\text{C}$ value decreases by 80 per mil from 10,800 to 9800 yr B.P. (12,500 to 10,000 cal yr B.P.); the decrease thus extends into the Preboreal (the earliest Holocene). This radiocarbon plateau occurs in both marine (8) and terrestrial (5) records and is referred to as the YD plateau. Our calibration shows that the YD plateau consists of two subplateaus at 10,000 and about 10,400 yr B.P.; the older one is characterized by a time of slow increase of the radiocarbon age. A similar decrease in $\Delta^{14}\text{C}$ of ~100 per mil (including magnetic effect) is observed from 12,600 to 12,100 yr B.P. (or 15,000 to 13,800 cal yr B.P.), which starts within the Oldest Dryas (OD) cold period and extends until nearly the end of the Allerød/Bølling

warm period. This plateau can be related to the radiocarbon plateau recorded in (non-varved) sediment cores from Switzerland (21). Our data strongly indicate a plateau around the OD cold period. It appears that the two radiocarbon plateaus in the YD and OD cold periods started a few centuries after the warm-to-cold transition. Furthermore, we also observe the millennium-scale fluctuations of about 100 per mil in $\Delta^{14}\text{C}$ before the OD; maxima at 16,000, 17,500, and 19,000 cal yr B.P.; and minima at 15,500, 17,000, 18,000, and 19,500 cal yr B.P.

When compared with changes in the atmospheric CO_2 concentration measured directly in polar ice cores (22) and reconstructed from South American peat (23), minima at 13,500 and 15,500 cal yr B.P. seem to respond to sharp increases in atmospheric CO_2 concentration. These coupled signals suggest that CO_2 degassed from the ocean, especially from the intermediate-deep ocean, induced the change of atmospheric $\Delta^{14}\text{C}$ because the ocean contains more than 90% of the global ^{14}C inventory and the oceanic C is depleted in ^{14}C . For a recent discussion concerning the connection of atmospheric ^{14}C and paleo-oceanographic parameters, we refer to (24). Paleo-oceanographic observations suggest that millennium-scale oscillations of the ocean thermohaline circulation (THC) occurred during the deglaciation (25). The THC oscillation can be linked to atmospheric $\Delta^{14}\text{C}$ as follows: $\Delta^{14}\text{C}$ increases when formation of North Atlantic Deep Water (NADW) is reduced abruptly and THC decreases, after climatic cooling such as the OD and YD cold periods; in contrast, $\Delta^{14}\text{C}$ decreases when THC northward heat ad-

Fig. 2. Atmospheric ^{14}C changes during the deglaciation (<20,000 cal yr B.P.), normalized to the present value and given in $\Delta^{14}\text{C}$ in per mil, reconstructed from annually laminated sediments of Lake Suigetsu, Japan. The symbols are as in Fig. 1. The features for the part overlapping the tree-ring record are excellent, including the wiggles in the radiocarbon calibration curve.

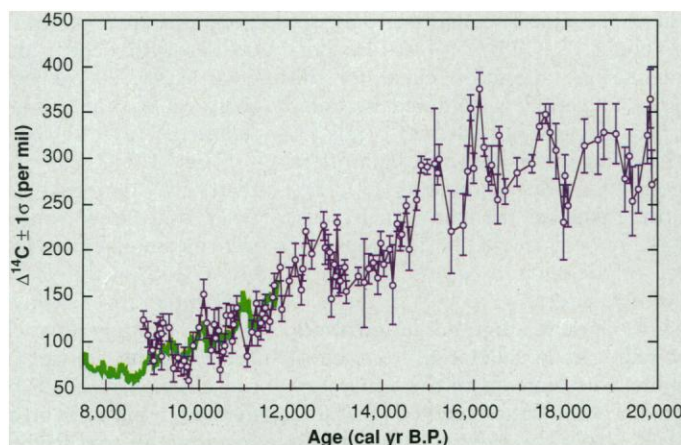
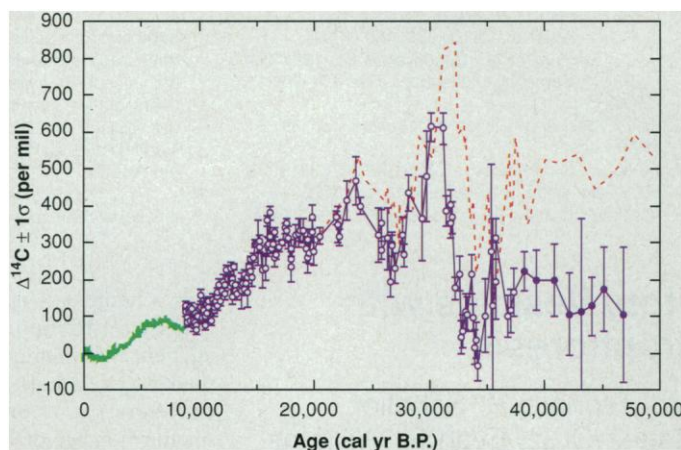


Fig. 3. Atmospheric $\Delta^{14}\text{C}$ changes beyond the Last Glacial Maximum. The symbols are as in Fig. 1. The absolute (calendar) ages older than $\sim 20,000$ yr B.P. should be considered as minimum ages. The red dashed line shows an instance with accumulated error of 2000 years at 40,000 cal yr B.P. in the varve chronology [see text and (12)]. The two peaks at 23,000 and 31,000 yr B.P. are superimposed on the long-term $\Delta^{14}\text{C}$ change, probably caused by geomagnetic field change.



vection and deep water production resume. Our atmospheric $\Delta^{14}\text{C}$ record implies that repeated cycles of such a process occurred, and a possibility that the NADW weakened for three or four periods during the last deglaciation is superimposed on the general trend of increasing ocean ventilation (26).

From the Last Glacial Maximum to 31,000 cal yr B.P., the long-term trend of $\Delta^{14}\text{C}$ agrees well with reconstruction of cosmogenic isotope production rate deduced by the ^{10}Be deposition reconstruction (19) and geomagnetic field intensity reconstruction (18) (Fig. 3). For this time span, we observe two pronounced peaks in $\Delta^{14}\text{C}$ at 23,000 and 31,000 cal yr B.P. The apparent $\Delta^{14}\text{C}$ increases correspond to an increase in the concentration of another cosmogenic isotope, ^{10}Be , at 23,000 and about 35,000 cal yr B.P., respectively, observed in ice cores from the Antarctic (27) and Greenland (28) as well as in marine sediments (29, 30). Furthermore, a ^{14}C anomaly at these times has been observed previously in speleothems, dated by both ^{14}C and U series (31). The time gap between the ^{14}C and ^{10}Be enhancements can be explained by errors in both varve and ice-core chronologies, as well as by the different geochemical behavior of these isotopes; ^{14}C is present in gaseous form (CO_2) and gradually diffuses in the Earth system, whereas ^{10}Be is a solid attached to aerosol particles and deposited with precipitation (32).

The broad increase in cosmogenic isotopes (both ^{10}Be and ^{14}C) at 23,000 yr B.P. can be explained as the increase in production rate by geomagnetic effects (28). The sharp ^{14}C peak we observed at $\sim 31,000$ yr B.P. is roughly 300 per mil in $\Delta^{14}\text{C}$ after removing the long-term trend. The ^{10}Be increases by a factor of 2 in ice cores during a period of ~ 2000 years (27). This factor of 2 increase corresponds to a ^{14}C increase by a factor of 1.3 or 300 per mil (33), which is exactly what we observe in our data. These

sharp enhancements in ^{10}Be and ^{14}C at the same time are too large to be explained by rearrangements of the C reservoirs on the Earth.

Increased cosmogenic isotope production caused by a nearby supernova explosion has been suggested as a cause for the drastically increased ^{10}Be levels at this time (29, 34). Another possible explanation is a magnetic excursion with a sharp change in inclination of the geomagnetic field and the implied concomitant decrease in the geomagnetic field strength. Such events are observed as the Mono Lake and Laschamp excursions, dated at 28,000 and 33,000 yr B.P. (uncalibrated), respectively (35). The sharp $\Delta^{14}\text{C}$ increase from Lake Suigetsu corresponds chronologically to the Mono Lake excursion. However, all of these explanations remain hypothetical.

The atmospheric radiocarbon calibration curve covering the past 45,000 years provides the basis for developing a better understanding of the past global C cycles and cosmogenic isotope production. Our high-resolution calibration curve is consistent with other proxies until 31,000 cal yr B.P. Beyond 31,000 cal yr B.P., much work is still needed to obtain a better understanding of the atmospheric $\Delta^{14}\text{C}$ signal. Here, our calibration deviates from paleomagnetic records (18, 20) and from recent combined U/Th and ^{14}C dating of speleothems (36). These data suggest that ^{14}C dates at this time are ~ 5000 years too young. This discrepancy can be caused either by speleothem dating problems (such as unknown initial ^{14}C age and possible detrital Th contamination) or missing varves in the older section of Lake Suigetsu. New ^{10}Be data from the Arctic GRIP and GISP2 cores show the large spike at $\sim 41,000$ cal yr BP (37), which is inconsistent with both our $\Delta^{14}\text{C}$ maximum and the Antarctic ^{10}Be record (27). This finding would indicate either a problem in one of chronologies, or

that the ^{10}Be and ^{14}C peaks do not have the same cause. Future work on the Lake Suigetsu core can help to solve the remaining questions.

REFERENCES AND NOTES

1. $\Delta^{14}\text{C}$ denotes the atmospheric $^{14}\text{CO}_2$ content, expressed as the per mil deviation of the ^{14}C content defined by the international oxalic acid standard after decay and fractionation correction [M. Stuiver and H. A. Pollach, *Radiocarbon* **19**, 355 (1977)].
2. The tree-ring calibration data are summarized in a special issue in M. Stuiver, A. Long, R. S. Kra, Eds., *Radiocarbon* **35** (1993).
3. B. Wohlfarth, *Quat. Sci. Rev.* **15**, 267 (1996).
4. I. Hajdas et al., *Climata Dyn.* **9**, 107 (1993); I. Hajdas et al., *Quat. Sci. Rev.* **14**, 137 (1995).
5. T. Goslar et al., *Nature* **377**, 414 (1995).
6. S. Björck et al., *Science* **274**, 1155 (1996).
7. E. Bard et al., *Nature* **345**, 405 (1990); E. Bard et al., *Radiocarbon* **35**, 191 (1993); E. Bard et al., *Nature* **382**, 241 (1996).
8. R. L. Edwards et al., *Science* **260**, 962 (1993).
9. K. A. Hughen et al., *Nature* **391**, 65 (1998).
10. cal yr B.P. expresses absolute years before the present, where the present is defined as 1950. Radiocarbon dates are expressed in yr B.P. (noncalibrated) with respect to 1950.
11. H. Kitagawa et al., *Radiocarbon* **37**, 371 (1995).
12. The SG core sediments from Lake Suigetsu were typically sampled per 90-cm-long section from one drilling hole, with the use of a so-called thin-wall sampler with piston. The recovered sediment is typically 85 to 90 cm long because of incomplete sampling or shrinking sediments. The sampling loss is typically less than 2 cm, corresponding to about 50 years during the glacial. Further details of the SG core are provided in (17). The accuracy is determined by sampling and varve counting errors. Based on the results of duplicated countings of selected sections, we determined the counting error to be less than 1.5%, corresponding to 150 years for 10,000 varves.
13. J. van der Plicht, A. T. Aerts, S. Wijma, A. Zondervan, *Radiocarbon* **37**, 657 (1995); A. Gott dang, D. J. W. Mous, J. van der Plicht, *ibid.*, p. 649.
14. To remove the possible contamination, we applied a strong acid-alkali-acid (AAA) treatment [W. G. Mook and H. J. Streuman, *FACT B*, 31 (1983)] to both samples and reference blanks. The blanks consisted of more than 50 ^{14}C -free plant materials, collected from the deep layer of the same SG core (corresponding to an age of about 90,000 to 100,000 years).
15. B. Kromer et al., *Radiocarbon* **38**, 607 (1996).
16. G. W. Pearson, *ibid.* **28**, 292 (1986).
17. H. Kitagawa and J. van der Plicht, paper presented at the 16th International Radiocarbon conference, Groningen, Netherlands, 16 to 20 June 1997.
18. Y. Guyodo and J.-P. Valet, *Earth Planet. Sci. Lett.* **143**, 23 (1996).
19. E. Bard, *Science* **277**, 532 (1997).
20. M. Frank et al., *Earth Planet. Sci. Lett.* **149**, 121 (1997); Y. Lao et al., *Nature* **357**, 576 (1992).
21. B. Amman and A. F. Lotter, *Boreas* **18**, 109 (1989).
22. J. M. Barnola et al., *Nature* **329**, 408 (1987); A. Neftel, H. Oeschger, T. Staffelbach, B. Staffer, *ibid.* **331**, 609 (1988).
23. R. A. Figge and J. W. C. White, *Global Biochem. Cycles* **9**, 391 (1995).
24. T. Wink and U. Siegenthaler, *Geophys. Monogr.* **32**, 185 (1985); T. F. Stocker and D. G. Wright, *Paleoceanography* **11**, 773 (1996); J. F. Adkins and E. A. Boyle, *ibid.* **12**, 337 (1997).
25. S. J. Lehman and L. D. Keigwin, *Nature* **356**, 757 (1992); C. D. Chales and R. G. Fairbanks, *ibid.* **355**, 416 (1992).
26. B. J. Haskell, T. C. Johnson, W. J. Showers, *Paleoceanography* **6**, 21 (1991); L. D. Keigwin et al., *J. Geophys. Res.* **96**, 16811 (1991).
27. G. M. Raisbeck et al., *Nature* **326**, 273 (1987).
28. J. Beer et al., in *The Last Deglaciation: Absolute and Radiocarbon Chronologies*, E. Bard and W. S.

- Broecker, Eds. (NATO ASI series, Springer-Verlag, Berlin/Heidelberg, Germany, 1992), pp. 141–153.
29. L. R. McHargue, P. E. Damon, D. J. Donahue, *Geophys. Res. Lett.* **22**, 659 (1995).
30. G. C. Castagnoli *et al.*, *ibid.*, p. 707.
31. J. C. Vogel, *Radiocarbon* **25**, 213 (1983).
32. H. Oeschger, in *Nuclear and Chemical Dating Techniques: Interpreting the Environmental Record*, L. A. Currie, Ed. (American Chemical Society, Washington, DC, 1982), pp. 5–42.
33. G. M. Raisbeck *et al.*, in (28), pp. 127–139.
34. C. P. Sonnett *et al.*, *Nature* **330**, 458 (1987).
35. J. C. Liddicoat *et al.*, *Geophys. J. Int.* **108**, 422 (1992); P. Vlag *et al.*, *J. Geophys. Res.* **101**, 28211 (1996).
36. J. C. Vogel and J. Kronfeld, *Radiocarbon* **39**, 27 (1997).
37. F. Yiou, *et al.*, *J. Geophys. Res.* **102**, 26783 (1997); R. C. Finkel and K. Nishizumi, *ibid.*, p. 26699.
38. We thank the Lake Suigetsu Scientific Drilling Team

led by Y. Yasuda, M Nishimura for the macrofossils collection from sediments; and E. R. M. Druffel and three anonymous reviewers for comments on the manuscript. This work was funded primarily by the Grant-Aid for Scientific Research (04214116) from the Ministry of Education, Science, and Culture (Japan) and partly by the Toyota Foundation (96-A-232).

1 October 1997; accepted 20 January 1998

Probing Single Secretory Vesicles with Capillary Electrophoresis

Daniel T. Chiu, Sheri J. Lillard, Richard H. Scheller, Richard N. Zare,* Sandra E. Rodriguez-Cruz, Evan R. Williams, Owe Orwar, Mats Sandberg, J. Anders Lundqvist

Secretory vesicles obtained from the atrial gland of the gastropod mollusk *Aplysia californica* were chemically analyzed individually with a combination of optical trapping, capillary electrophoresis separation, and a laser-induced fluorescence detection. With the use of optical trapping, a single vesicle that had attoliters (10^{-18} liters) of volume was introduced into the tapered inlet of a separation capillary. Once the vesicle was injected, it was lysed, and its components were fluorescently labeled with naphthalene-2,3-dicarboxaldehyde before separation. The resultant electropherograms indicated distinct variations in the contents of single vesicles.

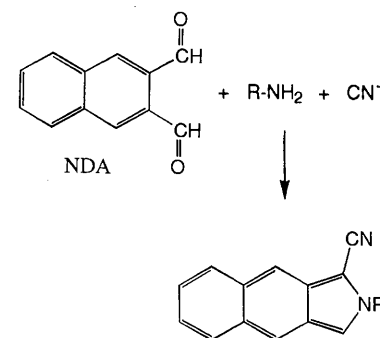
Biological messengers are synthesized intracellularly and packaged into secretory vesicles, where they are stored until a physiological signal triggers fusion of the vesicle membrane with the plasma membrane, resulting in the extracellular release of a chemical messenger. This mode of cellular signaling is used by all eukaryotic organisms in biological processes ranging from sensory perception to the regulation of reproductive cycles. Analysis of secretory products has been done on populations of vesicles, but the contents of a single vesicle are often sufficient to produce a biological response. Therefore, it is important to develop techniques of adequate sensitivity to characterize the array of chemical messengers within individual vesicles (1, 2). The sizes of vesicles range from 30 to 2000 nm, which corresponds to volumes from zeptoliters (10^{-21} liters) to low femtoliters (10^{-15} liters), respectively. The minute size of secretory vesicles makes their study by traditional analytical methods impossible.

Recently, capillary electrophoresis (CE) has emerged as a powerful separation technique for the analysis of ultrasmall sample volumes (3). A much pursued goal in the area of ultrasensitive chemical analysis is the use of CE to separate and analyze the contents of single biological vesicles (2). Using such methods, one can compare the contents of single secretory vesicles one at a time, revealing variations that would otherwise be buried within the analysis of populations. This type of study provides insight into the cellular mechanisms used to package and sort chemical messengers into vesicles and defines sets of secreted bioactive products with a precision previously unattainable.

Two considerations in the use of CE for the analysis of single vesicles are detection sensitivity (4) and sample introduction (5, 6). The sensitivity required to detect the laser-induced fluorescence (LIF) of a single dye molecule exists (4). Detection, however, is only the back half of the problem. Sample introduction and manipulation remain the primary challenge. Thus far, the analysis of single vesicles has been hindered by the difficulty of introducing a single vesicle into the separation capillary and analyzing its contents. Recently, the first part of this problem was overcome by the use of optical trapping and tapered capillaries (5). The second challenge is to label the contents of a single vesicle with a fluorophore for subsequent detection by LIF. In the present experiment, a miniature on-column derivatiza-

tion scheme was applied to the molecules under investigation. The key to ensure an efficient on-column reaction is to minimize the reaction volume, which leads to a higher concentration of analyte molecules and a smaller number of labeling molecules. The technique of tapered capillaries (5) also addresses this challenge. For example, the on-column reaction volume for a normal capillary inlet with an inner diameter (i.d.) of 25 μm and a length of 1000 μm is 4.9×10^{-10} liters. The reaction volume for a tapered capillary inlet of 1- μm i.d. of the same length, however, is 7.8×10^{-13} liters. This reduction in volume by a factor of 625 leads to a faster and more efficient reaction with fewer unreacted dye molecules. With this manipulation capability and improved reaction conditions, the contents of single biological vesicles can be probed, one by one.

The vesicles studied in this experiment were obtained from the atrial gland of the gastropod mollusk *Aplysia californica* (7). These vesicles contain bioactive peptides



that are packaged into secretory granules called dense core vesicles (DCVs) (8). These DCVs are large (average diameter $\approx 1 \mu\text{m}$) and can be easily isolated from *Aplysia*. This advantageous attribute of the DCVs has motivated their use in the present study. The atrial gland was first dissected from the distal end of the hermaphroditic duct, and subsequent slicing of the gland with a sharp razor blade released DCVs into a solution of artificial seawater. Most research on the atrial gland of *Aplysia* has been directed at the bioactive peptides (9), which are involved in this animal's reproductive behavior. Therefore, it is interesting to find in the present study that the DCVs also contain large amounts of primary amine-containing compounds of

D. T. Chiu, S. J. Lillard, R. N. Zare, Department of Chemistry, Stanford University, Stanford, CA 94305, USA.
R. H. Scheller, Department of Molecular and Cellular Physiology, Howard Hughes Medical Institute, Stanford University, Stanford, CA 94305, USA.
S. E. Rodriguez-Cruz and E. R. Williams, Department of Chemistry, University of California, Berkeley, CA 94720, USA.
O. Orwar and J. A. Lundqvist, Department of Chemistry, Göteborg University, SE-412 96, Göteborg, Sweden.
M. Sandberg, Department of Anatomy and Cell Biology, Göteborg University, SE-413 90, Göteborg, Sweden.

*To whom correspondence should be addressed.